Monthly Notices
of the
ROYAL ASTRONOMICAL SOCIETY

MNRAS **505,** 5567–5583 (2021)
Advance Access publication 2021 May 22

https://doi.org/10.1093/mnras/stab1481

Red Be stars in the Magellanic Clouds?

Katherine Vieira,[1,2]★ Alejandro García-Varela,[3]★ Beatriz Sabogal,[3] Leandro Rocha Rímulo[3] and Jesús Hernández[4]

[1]*Instituto de Astronomía y Ciencias Planetarias INCT, Universidad de Atacama, Copayapu 485, Copiapó, Chile*
[2]*Centro de Investigaciones de Astronomía, Apartado Postal 264, Mérida 5101-A, Venezuela*
[3]*Universidad de los Andes, Departamento de Física, Cra. 1 No. 18A-10, Bloque Ip, AA 4976, Bogotá, Colombia*
[4]*Instituto de Astronomía, UNAM, Unidad Académica en Ensenada, Ensenada 22860, México*

Accepted 2021 May 18. Received 2021 April 14; in original form 2019 October 31

ABSTRACT

We revisit the subject of Be candidate stars towards the Magellanic Clouds, previously studied by the authors using SPM4 proper motions. We obtain *Gaia* DR2 parallaxes and proper motions for 2357 and 994 LMC and SMC Be candidates, respectively. Parallaxes and proper motions versus colour $V - I$ easily reveal the presence of the redder galactic contaminant foreground, as concluded in our previous work, but this time we do find a few red Be candidates consistent with being true Magellanic objects. A membership assessment to each Magellanic Cloud is done for each Be candidate, based on the distribution of their parallaxes and proper motions. From a compilation of published catalogues of spectroscopically confirmed emission line stars,we find that 41 (LMC) and 56 (SMC) of the Be candidates have shown the H_α line in emission. Near-infrared IRSF *JHKs* magnitudes are obtained for about 70 per cent of the Be candidates with *Gaia* DR2 astrometric data. Mid-infrared SAGE IRAC 3.6, 4.5, 5.8, and 8.0 μm magnitudes are obtained for about 85 per cent as well. After discarding possible Herbig Ae/Be stars, one LMC and three SMC B emission line confirmed stars show significantly redder optical, near- and mid-infrared colours than what has been typically measured for Classical Be stars – they are called red Be stars. Taking into account that classical Be stars do not show these red colours, further studies about these four stars are needed in order to establish their true nature and explain the observed red excess.

Key words: parallaxes – proper motion – stars: emission-line, Be – Magellanic Clouds.

1 INTRODUCTION

Be stars are broadly defined as non-supergiant (luminosity class II to V) B-type stars that have or have had Balmer emission lines (Collins 1987). The presence of a flattened circumstellar gaseous disc formed of material ejected from the star, a dust-free Keplerian *decretion disc*, is currently the accepted explanation for some of the observed features in Be stars: the UV stellar light is reprocessed in it and produces the emission lines, and the observed infrared (IR) excess and polarization result from the scattering of the stellar light by the disc (see Rivinius et al. 2013 for details). Several mechanisms have been proposed for the mass-ejection process that forms the disc, which are well constrained but not totally understood. In the so-called Classical Be (CBe), it clearly comes from the rapid rotation of the star, probably along with other processes including non-radial pulsations and small-scale magnetic fields. In binary stars, the material is being accreted by the companion of the Be star, generally a white dwarf.

Mennickent et al. (2002) and Sabogal et al. (2005) have identified a large number of Be candidate stars towards the Magellanic Clouds based on their photometric variability in the OGLE-II *I*-band. Paul et al. (2012) showed that this photometric method is effective in the selection of Be candidates, as their spectroscopic analysis found that most of the stars studied from a sample of such candidates in both LMC and SMC belong to early-type stars with emission supporting circumstellar material. However, an enigmatic subgroup in the LMC sample was found and proposed as a possible subclass of stars that needed further analysis. In Vieira et al. (2017), we proved that this subgroup was in fact Galactic foreground contamination, as revealed by their SPM4 (Girard et al. 2010) proper motions. In the SMC, only a few contaminants were found.

In this investigation, the results in Vieira et al. (2017) are tested with *Gaia* DR2 (Gaia Collaboration 2016, 2018a), which has significantly better proper motions and also measured parallaxes that were not available before. The main result regarding the redder candidates being contaminants was indeed confirmed, but several red Be candidates emerged as true Magellanic stars. Though most of them are classified as Type 4 (see Mennickent et al. 2002 for this classification, according to their variability light-curve morphology) and are considered by them and other references as surely CBe stars, they do not occupy the IR versus optical colours known so far for Be stars.

This paper goes through the following topics: cleaning the Be candidates and matching with *Gaia* DR2 (Sections 2 and 3), statistical analysis of their parallaxes and proper motions and membership assessment (Sections 4, 5, and 6), crossmatch with spectroscopic catalogues to obtain the list of spectroscopically confirmed B emission line (BEL) stars (Section 7), distribution of the light curve variability types of Be candidate and BEL stars (Section 8), near- and mid-IR photometry and finding redder than expected

★ E-mail: katherine.vieira@uda.cl (KV); josegarc@uniandes.edu.co (AG-V)

Magellanic confirmed BEL and Be candidate stars (Section 9), some alternative explanations for the results (Section 10), and conclusions (Section 11). Through this paper, we use the following expressions: Be candidate stars, to indicate stars that were selected as such in the references consulted because of their photometric properties, in particular variability; and confirmed BEL, to indicate stars that have been previously reported as B stars with the H_α line in emission, and that are a subset of the Be candidate ones.

2 CLEANING THE BE CANDIDATES

Be candidate stars for the LMC and SMC were obtained from Sabogal et al. (2005) and Mennickent et al. (2002), respectively, where a total of 2446 and 1019 candidates are listed. In Vieira et al. (2017), we had found a few repeated entries in each catalogue, with the same OGLE II identification, but in this reanalysis, we found that OGLE II has a slightly larger set of very similar entries, all correspond to pairs of stars, and located less than 2 arcsec from each other, with very similar photometry (<0.1 magnitude differences) in the three *BVI* bands. These are repeated entries with bad enough astrometry to end up listed as different stars instead of the same and in many cases, they have different OGLE II identifications (which is based on their coordinates). One entry per pair was kept (the first one listed), so the clean lists of Be candidates have 2393 and 1004 stars, towards the LMC and SMC, respectively.

3 CROSSMATCHING WITH *Gaia* DR2

To properly crossmatch the Be candidates with *Gaia* DR2, we considered closeness not only in sky position but also in photometry, since the *Gaia* DR2 *G*-band is close enough to the OGLE-II *V*-band, as to serve to clean up possible misidentifications. *Gaia* DR2 is significantly deeper in magnitude, therefore denser than OGLE-II, so there are chances for incorrect matches (see Fig. 1). This approach is supported by the fact that among the only-positional matches up to 4 arcsec, a clear concentration of data points at $V - G \sim 0$ is visible.

In the SMC, at least one *Gaia* DR2 match was found within 2 arcsec that also looked close enough in photometry, but in the LMC, for a few stars the best looking match was almost as far as 4 arcsec. The *Gaia* DR2 match was chosen as the star having the lowest value of

$$\text{posmag\_ranking} = \sqrt{\left(\frac{\Delta\theta}{\theta_{\max}}\right)^2 + \left(\frac{V-G}{1\text{mag}}\right)^2}, \quad (1)$$

where $\Delta\theta$ is the sky angular separation in arcseconds between the (RA, DEC) coordinates listed for the Be candidates and the *Gaia* DR2 ones, $\theta_{\max} = 2$ arcsec for the SMC and $\theta_{\max} = 4$ arcsec for the LMC. As the equation above suggests, posmag_ranking is defined to measure the closeness in both sky position and visual photometry. All entries in the clean lists of Be candidates have a *Gaia* DR2 match, but we believe that those few with $|V - G| \sim 1$ mag or $\Delta\theta >$ 3 arcsec are mismatches, as suggested by Fig. 1. We do not discard any star for this reason, but we do keep in mind that they could be mismatches. We keep the posmag_ranking value for future reference.

4 FIRST ANALYSIS FROM PARALLAXES AND PROPER MOTIONS

Of the 2393 and 1004 *Gaia* DR2 matches for the LMC and SMC Be candidates, only 2357 and 994, respectively, have parallaxes and proper motions measured in *Gaia* DR2, and with these data sets, we will perform the rest of the analysis. Fig. 2 clearly reveals the already

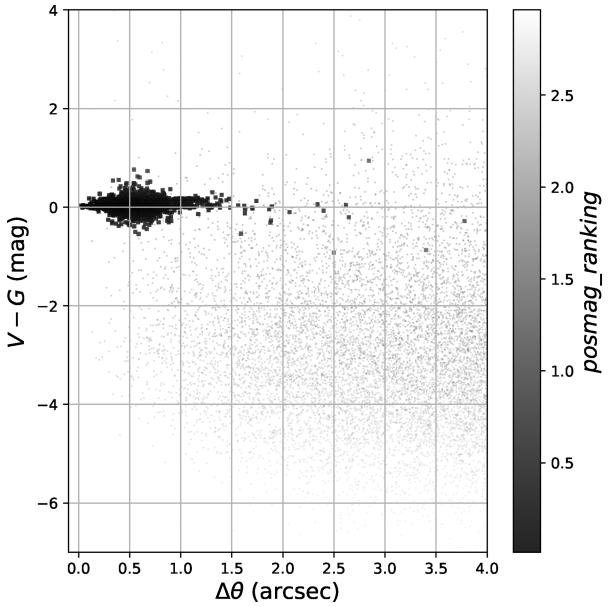

Figure 1. Matches between LMC Be candidates and *Gaia* DR2. This plot of $V - G$ versus $\Delta\theta$, colour-coded by *posmag_ranking*, for the *Gaia* DR2 entries chosen as matches for the Be candidates (filled circles), suggests that except for a few outliers beyond $\Delta\theta \sim 2.7$ arcsec, the vast majority (99.8 per cent) of these identifications are correct. Positional-only matches within 4 arcsec (light dots) are plotted as well, many of them are nearby fainter stars in *Gaia* DR2, and illustrate why *posmag_ranking* is best to choose the true match in *Gaia* DR2.

known result from Vieira et al. (2017): there is a group of red stars ($V - I \gtrsim 0.6$) having parallaxes and proper motions that clearly puts them as a foreground population residing in the Milky Way, while the bluer portion of the candidates does exhibit the corresponding expected values for the Magellanic Clouds. Nonetheless, not all of the red Be candidates belong to the foreground population; there are $V - I \gtrsim 0.6$ objects that reside in the Magellanic Clouds. This result arises clearly thanks to the manyfold improvement in proper motion precision and accuracy of *Gaia* DR2, compared to SPM4's capabilities, that beats down errors to the point of allowing a clear separation of these two populations. As expected, despite some overlap, stars belonging to the Magellanic Clouds do exhibit a significantly larger concentration of their values of proper motion, which are further confirmed by parallaxes. In fact, for a few blue Be candidates, it looks like their membership to the Magellanic Clouds could be reconsidered. Not surprisingly, many of the candidates belonging to the Magellanic Clouds have larger errors, because of their significantly larger distance. But this feature is indeed a piece of valid information to consider when assessing the membership of a Be candidate to these neighbour galaxies. As opposed to the usual approach where large error data are discarded in order to get clean samples, in this work rejecting large-error data is in fact counterproductive. On the other hand, since membership to a population is significantly decided by its closeness to the mean value of the population, larger error data hinder finding that mean value with precision.

5 DEALING WITH ERRORS TO FIND A GOOD SAMPLE OF MAGELLANIC BE CANDIDATES

The LMC and SMC absolute proper motions have been measured from the ground (e.g. Vieira et al. 2010) and space (with *Gaia*

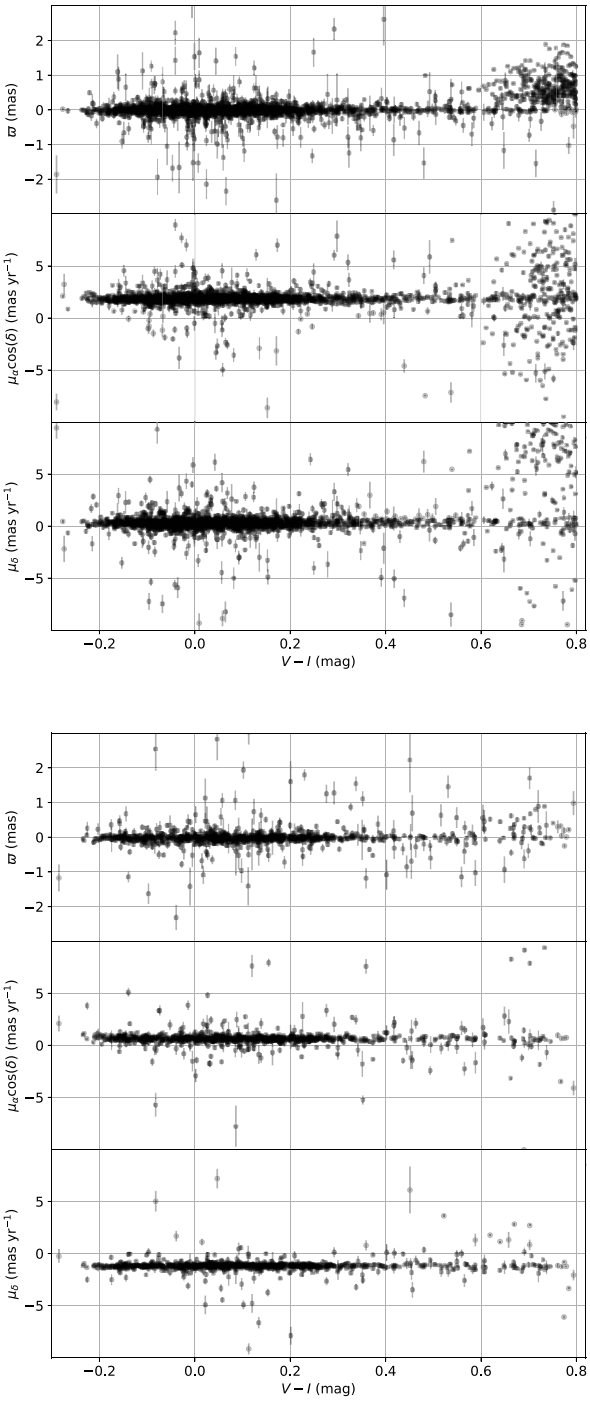

Figure 2. *Gaia* DR2 Parallaxes and proper motions with their respective error bars for the LMC (upper panel) and SMC (lower panel) Be candidates versus $V - I$ colour.

DR2 itself, Gaia Collaboration 2018b). Despite their small value as compared to Milky Way disc stars, for example, measuring the angular displacement in the sky per unit time of the Magellanic Clouds ($\sim$2 mas yr^{-1}) is a perfectly doable task for *Gaia* DR2, given its proper motion mean precision of 0.06–0.15 mas yr^{-1} for sources with $G < 17$. Parallax is a different issue, as the LMC and SMC distances ($\sim$ 50 and 60 kpc, respectively) translate into parallaxes measurements of 20 and 16 μas, and *Gaia* DR2 parallax errors are about 40–90 μas for sources with $G < 17$ (Luri et al. 2019). Given

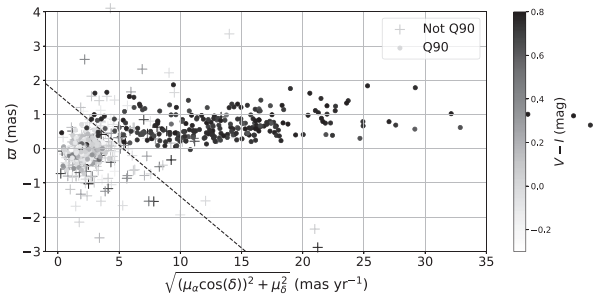

Figure 3. Plot corresponding to steps (ii) and (iii) for the LMC. Stars to the left of the dashed line are selected in step (iii) as sample LMC1. Stars to the right of the line are red in $V - I$ and have large total proper motions; they are mostly Milky Way foreground stars. Data not in sample LMC Q90 (crosses) have large errors but they cluster around the LMC mean value, though with a much larger dispersion.

these circumstances, we decided to follow this approach, only to find the mean value of parallax and proper motions of the LMC and SMC:

(i) Select the sample with all stars below the 90th quantile of proper motion error in both coordinates (from now on, samples LMC/SMC Q90).

(ii) Plot parallax ϖ versus total proper motion $\sqrt{(\mu_\alpha \cos\delta)^2 + \mu_\delta^2}$, colour coded by $V - I$ (see Fig. 3).

(iii) From this plot, select the cluster of data corresponding to the LMC or the SMC that is visibly separated from the foreground population by their clustering in the plotted data and also the distribution of their $V - I$ colour (from now on, samples LMC1/SMC1). For example, LMC1 is defined as all stars in LMC Q90 to the left of the dashed line plotted in Fig. 3. Similarly happens for SMC1.

(iv) Apply a quantile–quantile or Q–Q plot on ϖ, $\mu_\alpha \cos\delta$, and μ_δ for samples LMC1/SMC1 to determine the mean and dispersion values for these data.

(v) Adopt the obtained mean value for each measurement as the population mean of each Magellanic Cloud.

Fig. 3 illustrates steps (ii) and (iii) for the LMC, and the separation of the two populations is clear and evident, when the colour information is considered. In step (iv), the Q–Q plots are computed with respect to a standard normal distribution $N(0, 1)$, so if the data do follow a normal distribution, the Q–Q plot will look like a straight line where the y-intercept indicates the mean value and the slope corresponds to the dispersion. As visible in Fig. 4, showing the Q–Q plots of $\mu_\alpha \cos\delta$ and μ_δ for the LMC1 sample, the 10 per cent extreme data points at each side were not considered for the fit. It is visible that those extreme points deviate visibly from the straight line (the tails of the distribution are heavier than normal), which is not entirely unexpected. Besides some contamination from foreground stars, the observed dispersion is mostly caused by error measurements and the samples studied have data of various quality. Since the points used in the fit do follow very closely a linear relation and the LMC1 and SMC1 data sets have symmetrical distributions in the Q–Q plots, the obtained mean values are very robust. Similarly happens for parallaxes in both LMC and SMC. Resulting mean and dispersion values are listed in Table 1.

It can be noticed that the mean parallax value is negative for both Clouds and significantly enough compared to their dispersions. *Gaia* DR2 parallaxes are known to have an offset towards smaller than real values (*Gaia* DR2 $-$ true value <0) for an amount that has been computed, among others, to be -0.082 ± 0.033 using eclipsing binaries (Stassun & Torres 2018), -0.0528 ± 2.4 (stat.)$\pm$1(syst.)

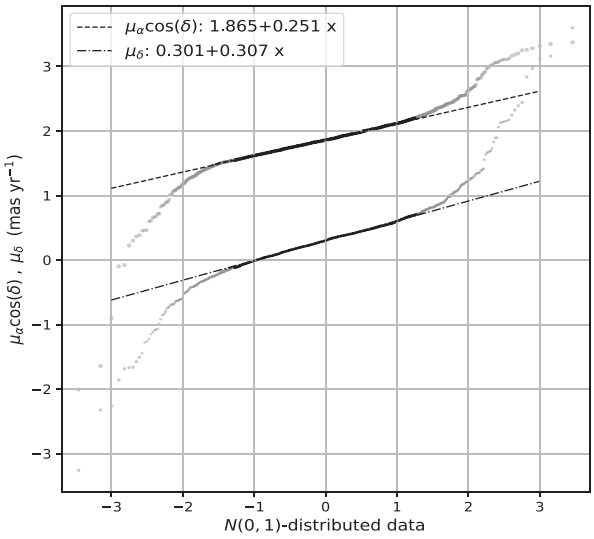

Figure 4. Q–Q plots result for the LMC proper motions on the sample LMC1. For the Q–Q fit, 10 per cent extreme data at each side (grey symbols) are not considered.

Table 1. Mean and dispersion values of parallax and proper motions for LMC and SMC Be candidates, as obtained from Q–Q plots on samples LMC1 and SMC1.

	Sample size	ϖ (mas)	$\mu_\alpha \cos\delta$ (mas yr^{-1})	μ_δ (mas yr^{-1})
LMC1	1856	-0.015 ± 0.081	1.865 ± 0.251	0.301 ± 0.307
SMC1	872	-0.023 ± 0.075	0.680 ± 0.202	-1.220 ± 0.141

mas using red giant branch and Helium-burning red clump stars (Zinn et al. 2019), and the official value using quasars given by the Gaia Collaboration of −0.030 mas (Luri et al. 2018). In the LMC, such offset has been found to have in fact systematic periodic variations (see fig. 13 in Arenou et al. 2018). Our results are within this range of biases, as compared to the expected parallaxes of 0.020 and 0.016 mas for the LMC and the SMC, respectively. It is not of concern what the mean values are for each Cloud, as we use them only to separate Magellanic Be candidates from foreground population, based on the clustering of the data.

As for the measured dispersion, in all the three kinds of data, within each Cloud, the intrinsic expected cosmic dispersion is substantially smaller than the observed one. For the young population in the Magellanic Clouds, velocity dispersion has been measured to be as low as 6 km s^{-1} (Gyuk et al. 2000). A 15 km s^{-1} velocity dispersion at 50(60) kpc yields a proper motion dispersion of 0.06(0.05) mas yr^{-1}. Therefore, the observed variance is caused dominantly by measurement errors.

6 DATA STANDARDIZATION AND MEMBERSHIP ASSESSMENT TO THE LMC/SMC

When the dispersion of a univariate sample of data is dominated by the measurement errors, the non-constant scale of these data produces problems trying to analyse them. In order to obtain a unique scale for the data, the standardization of data (Feigelson & Babu 2012, p. 193) is widely used in the statistics and astrostatistic context, using the formula given by

$$\text{datum}_{\text{norm}} = \frac{\text{datum} \ - \text{population mean}}{\text{datum}_{\text{error}}}.$$

This standardization process should yield a normal standard $N(0, 1)$ distribution. Extended explanations of this method can be found in Patel & Read (1996, p. 19), Heiberger & Holland (2015, p. 50), and Heumann et al. (2016, p. 19).

If the dispersion S of the normalized data is significantly $\neq 1$, a scaling of the errors *may* solve the problem, revealing that original quoted errors were under- ($S > 1$) or overestimated ($S < 1$). This works and must work for all individual errors, whether large or small. We computed normalized data for all the LMC and SMC stars, using the mean values obtained from LMC1 and SMC1, respectively. A plot of the individual data error versus the normalized data, as seen in Fig. 5 for the LMC stars, reveals in first place the expected concentration around zero for stars that truly belong to the LMC, while foreground Galactic stars behave visibly differently, both in mean and dispersion of the normalized data, and foreground stars have a huge dispersion that is in fact mostly cosmic. Sample LMC Q90 containing stars well measured in proper motions include both Magellanic Clouds stars and also Milky Way ones, the latter easily visible with large values of normalized data. Sample LMC1 concentrates around zero, and so does sample 'not LMC Q90', which highlights once again how using normalized data allows us to keep these data that behave like members of the Magellanic Clouds, despite having larger individual errors. These larger error data follow the mean of the LMC though with a larger dispersion than for the LMC1 sample but still significantly smaller than the dispersion of foreground stars. Similarly happens with the SMC data though the foreground population is significantly lesser, as we already know. Q–Q plots on the normalized data for the LMC1 and SMC1 samples, which we consider are constituted by single LMC and SMC populations, respectively, show that for these samples the individual errors are all underestimated by at least the corresponding dispersions found (results in Table 2). As before, the 10 per cent extreme data showed a higher slope indicative of a higher scaling needed to *standardize* the data. The true underestimation factor may not be as uniform as a single scale value even across the LMC1 and SMC1 samples, and it is certainly not enough for the data outside them that could suffer from even larger underestimations.[1] This – again – is not entirely unexpected, as the proper *Gaia* consortium has warned of error underestimation in the *Gaia* DR2 data (Gaia Collaboration 2018a).

6.1 Membership assessment

As the scaling factor for the data individual errors is not uniform across the Magellanic data, using the obtained scales with the LMC1 and SMC1 samples, to *standardize* the whole normalized data sets and use a normal standard probability distribution $N(0, 1)$ as a model of the Magellanic populations on such data, is not entirely correct. And though these standard data help not to lose real Magellanic stars because of their individual larger errors/dispersion, there is also the issue of how to model the distribution of the foreground Galactic population in those same variables. The general approach is to model

[1] With the largest possible LMC/SMC population sample, the slopes of the Q–Q plots at each normalized datum can in fact be taken as the scaling factor for the corresponding individual error. That would effectively fully *standardize* that sample.

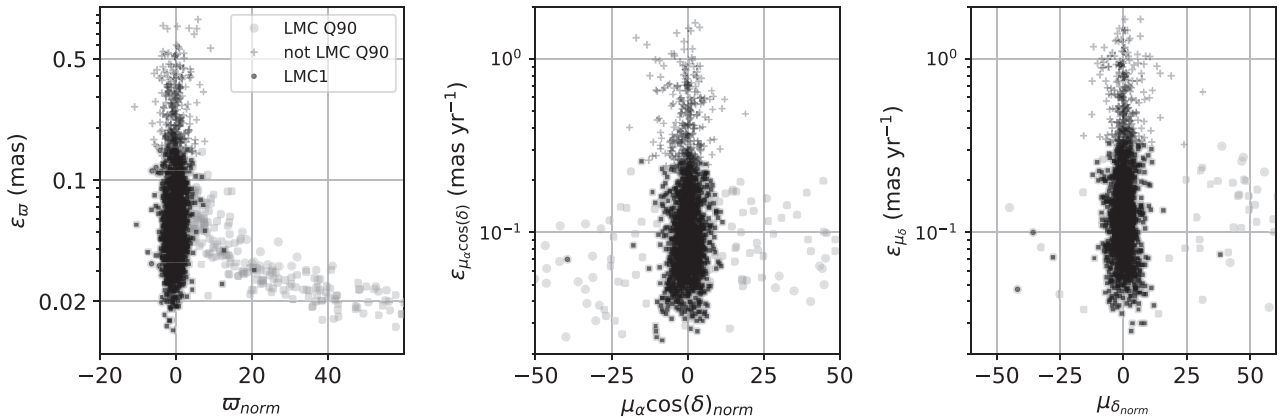

Figure 5. Individual data errors versus normalized data for LMC Be candidates. Despite their larger errors, data not in sample LMC Q90 (crosses) cluster around the LMC mean values (zero) in normalized variables, the same way best measured LMC1 data do. Discarding larger error data from start would systematically bias the obtained samples of Magellanic Clouds stars.

Table 2. Mean and dispersion values of normalized parallax and proper motions (which are unitless), as obtained from Q–Q plots, for samples LMC1 and SMC1.

	Sample size	$\varpi_{\rm norm}$	$\mu_\alpha \cos\delta_{\rm norm}$	$\mu_{\delta norm}$
LMC1	1856	-0.036 ± 1.522	-0.041 ± 2.865	0.038 ± 2.707
SMC1	872	-0.042 ± 1.534	0.039 ± 1.989	0.020 ± 1.801

the expected frequency of stars for each of the populations present in the chosen variables, and then the probability to belong to a given population is the ratio of its expected frequency over the sum of the same for all the populations present. A model for the latter is not an easy task because of varying systematic trends in proper motion data caused by, e.g. solar motion or galactic rotation; also, clusters populations may distribute themselves following a non-normal or non-symmetric distributions. Parametric (e.g. the seminal paper by Vasilevskis et al. 1958) and non-parametric approaches (e.g. Galadí-Enríquez et al. 1998) have been devised to treat this issue.

In the SMC, where we already know that contamination is less, a plot of the standardized proper motions for all the SMC data shows a clear concentration of data points within a unitless distance of 15 from (0,0), which we call sample SMC2 (976 stars), well isolated from a few scattered stars at distances larger than 20 from the origin. This same cut does not look as clean in the LMC (sample LMC2, 2116 stars) where contamination is larger and Milky Way stars overlap more with the LMC population (see Fig. 6). Interestingly, the above cut in standardized proper motions is enough to automatically select stars with standardized parallaxes close to zero, as seen in Fig. 7. The other way around, that is selecting first by standardized parallaxes is more visibly affected by foreground contamination.

In any case, Magellanic stars cluster around zero simultaneously in standardized parallax and proper motions. This leads us to define a new variable χ, as follows:

$$\chi = \sqrt{\left(\varpi_{std}\right)^2 + \left(\mu_\alpha \cos(\delta)_{\ std}\right)^2 + \left(\mu_{\delta\ std}\right)^2}$$

which should follow closely a χ (Chi) distribution with 3 degrees of freedom (Evans et al. 2000, p. 57). Such probability distribution has a mode at $\chi = \sqrt{2}$, and $\chi \leq 3.389$ should enclose 99 per cent of the Magellanic population, if all standardized data truly followed $N(0, 1)$ distributions and were also free of contamination . Fig. 8

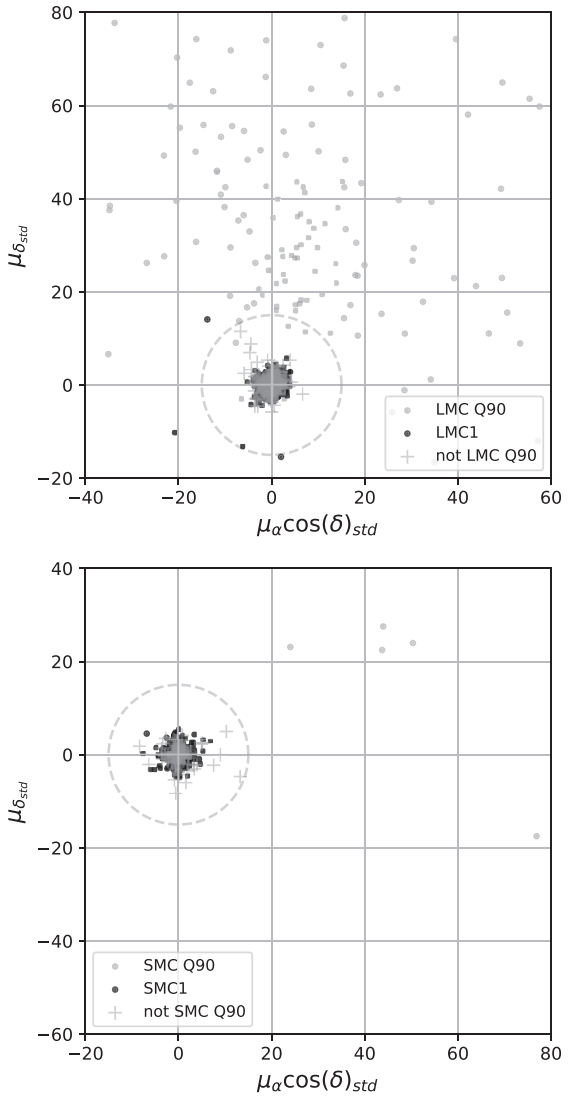

Figure 6. Standardized proper motions of the Be candidates towards the LMC (upper panel) and the SMC (lower panel). In the SMC, the cut at radius = 15 from the origin (sample SMC2) cleanly separates Magellanic from foreground population. This same limit applied to the LMC (sample LMC2) does not work as neatly due to larger and overlapping foreground contamination.

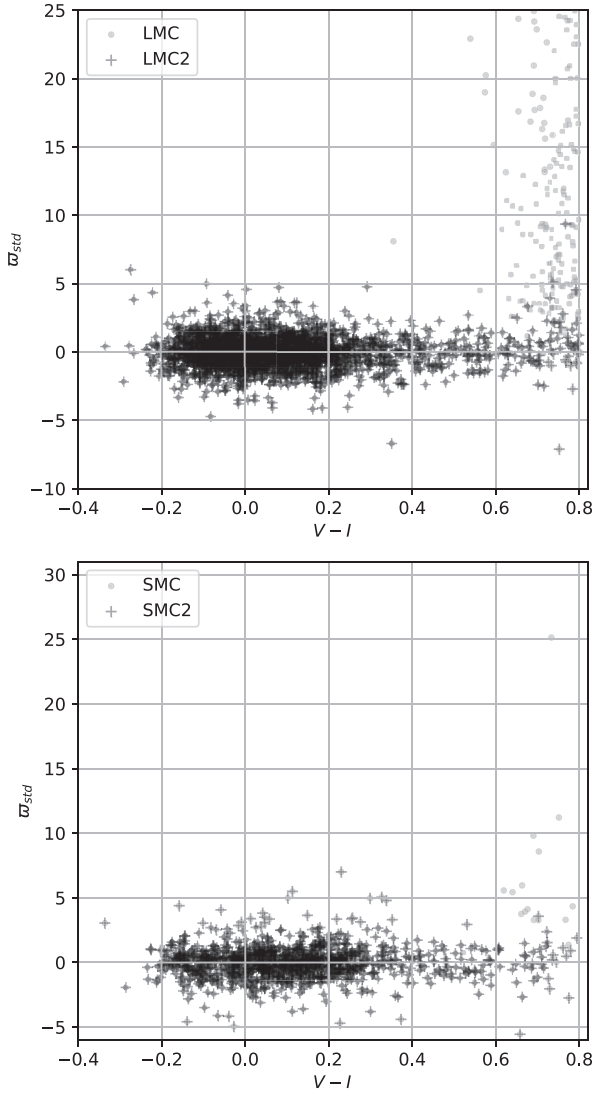

Figure 7. Standardized parallaxes of the Be candidates towards the LMC (upper panel) and the SMC (lower panel) versus $V-I$. Black crosses correspond to samples LMC2 and SMC2, chosen solely from their standardized proper motions.

plots χ versus $V-I$ for the LMC and SMC data, and from the distribution of both the bluer Magellanic population and the redder Galactic one, we decide to draw a limit between the two at $\chi = 10$. We believe that incomplete standardization of the most extreme data within the Magellanic populations has caused them to stray beyond the expected values for the χ distribution. Contamination can also play a role, but we expect it to be minimal at low values of χ, as shown by the histogram of χ for the whole LMC and SMC data (see inset in Fig. 8) that clearly shows Magellanic stars clustering around $\chi = \sqrt{2}$, and a secondary peak much farther away obviously caused by Milky Way stars. In any case, our standardized data are good in a relative sense, since Galactic foreground stars distribute themselves visibly far away from the cluster of Magellanic data points around zero. In other words, the data themselves have indicated us where to do the final cut to select the best possible single population LMC and SMC samples, that is all stars with $\chi < 10$, which yields samples LMC3 (2109 stars) and SMC3 (974 stars).

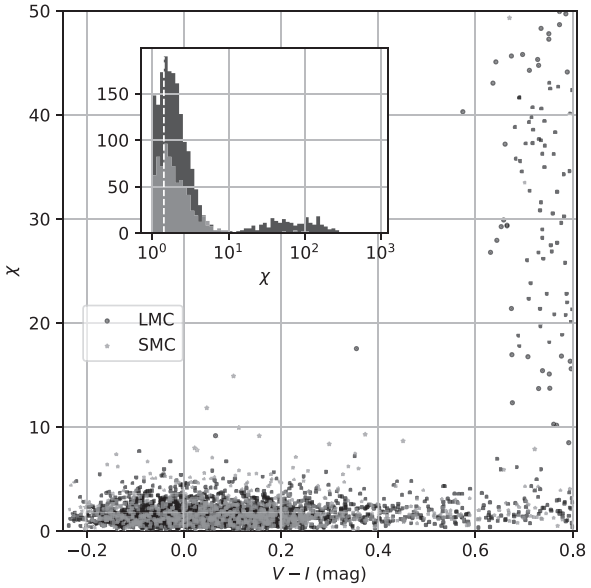

Figure 8. Plot of χ values versus $V-I$ for the LMC (black) and SMC (grey) Be candidates. From the distribution of the data points for both Clouds, we put $\chi = 10$ as limit to separate Magellanic populations from Galactic ones. Inset figure shows the histogram in a log-scale of χ values that encompasses all Be candidates; Galactic stars can be seen occupying a very extended range in χ. The vertical white dashed line marks $\chi = \sqrt{2}$, the mode for a χ distribution with 3 degrees of freedom.

Using χ as we just did implies that we are considering the three types of standardized data as independent. We must mention at this point that we did observe some slight correlation between the normalized parallax and proper motions, though not among the proper motions. These correlations were visibly reduced – but still a bit visible – in the standardized data (because the scaling did not work for all data, as we explained above, see Fig. 9). We believe that our assessment is nonetheless precise enough for the purpose of our investigation, correctly separate Magellanic stars from the Galactic ones.

When plotting the original ϖ, $\mu_\alpha \cos(\delta)$, and μ_δ data versus $V-I$ colour for the LMC3 and SMC3 samples, there appear to be some blue outliers that do not concentrate around the LMC/SMC mean value as much as the rest of the data. We have concluded that their error bars are substantially larger than what is quoted by *Gaia* DR2, and that would explain their apparent random distant location from the mean. We do in fact found that blue stars in the Be candidates have systematically larger errors than red ones in *Gaia* DR2, but it could be caused precisely by the dominance of LMC/SMC stars in that colour, which because of their distance are more difficult to measure.

7 CROSSMATCH WITH SPECTROSCOPIC CATALOGUES

Our lists of Be candidates were crossmatched with several previous publications and online databases of spectroscopically confirmed Be stars towards the Magellanic Clouds area, listed in Table 3. Despite these stars are called Be stars in those works, they are in many cases BEL stars at the time of observations and not necessarily CBe. The crossmatch radius used was 2.5 arcsec, but the vast majority of our Be candidates were matched within 1 arcsec. A few of our Be candidates appear simultaneously in several of these catalogues, because they

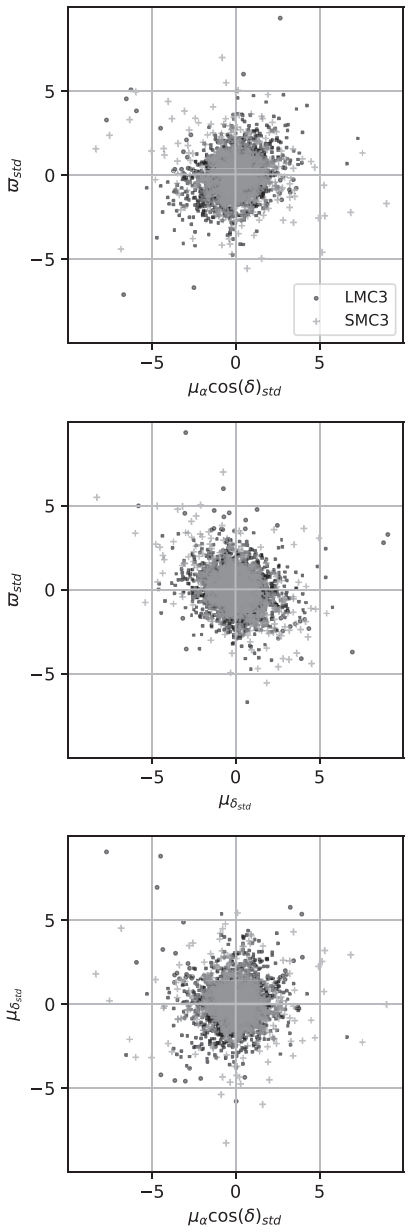

Figure 9. Correlations in standardized parallaxes and proper motions of the Be candidates in the LMC3 (black) and SMC3 (grey) samples. Parallax and proper motions look a bit correlated though proper motions not among themselves.

have common stars among them. Only one Be candidate in the SMC (ID = 3) was matched to two different confirmed BEL stars, *smc1-10* and *smc2-12* in Paul et al. (2012), which in that publication have the same coordinates and OGLE data, but different radial velocity measurements, though similar within their error bars. The stars also have very similar spectral range. Whichever is the correct match, both are confirmed BEL stars.

A total of 41 of our LMC Be candidates have a confirmed BEL star match and so do 56 of our SMC Be candidates. All of the confirmed BEL stars belong to the Magellanic Clouds according to our criteria $\chi < 10$ (LMC3/SMC3 samples), except one (ID = 462 in LMC) that has no *Gaia* DR2 data and therefore no value to decide its membership to the LMC. Also, all of the confirmed BEL stars have $|V - G| < 1$ and $\Delta\theta < 2.7$ arcsec; therefore, their *Gaia* DR2 data are most surely true matches.

Examining the confirmed BEL stars sample in more detail, we find that they all have $\chi < 4.5$ except two stars in the SMC: ID = 55 ($\chi = 7.4$) and ID = 798 ($\chi = 9.2$), which are both red in optical $V - I > 0.35$, and both have the largest errors and deviations from the mean value in all parallaxes and proper motions in this sample. Star ID = 55 has a duplicate flag in *Gaia* DR2. Among the SMC confirmed BEL stars, the following IDs have a duplicate flag in *Gaia* DR2: 55, 85, 88, 89, 103, 284, and 331, and the only one LMC confirmed BEL star with such a flag is ID = 684.

A crossmatch with SIMBAD was performed as well to explore how our Be candidates were classified in it. SIMBAD is a highly non-uniform database that contains a lot of information for some stars but none about many others. A crossmatch within 3 arcsec with our lists of Be candidates showed in several cases multiple matches. Keeping the closest match, we found that most of the stars were classified (under Object Type) as variable, a portion of them as Be stars, others as Long Period, Ellipsoidal and Eclipsing variables, etc. Verifying the certainty of these classifications is beyond the scope of this paper; it simply illustrates that a portion of our Be candidates can in fact be other types of variables, which is not entirely unexpected.

8 OGLE-BASED VARIABILITY CLASSIFICATION OF THE BE CANDIDATE AND CONFIRMED BEL STARS

Our Be candidates have a classification in Types 1–4, proposed by Mennickent et al. (2002), based on their OGLE *I*-band light curves morphology: Type 1 stars show outbursts, Type 2 stars show high and low states, Type 3 stars show periodic variations, and Type 4 stars show stochastic variations. There are stars that behave like Type 1 and Type 2 simultaneously and are classified as Type 1/2. In our study, only the LMC has the latter.

Table 4 shows how many stars per Type are in the LMC3/SMC3 samples and also how many of these are confirmed BEL stars. It reveals that confirmed BEL stars can be found in all types, but they are more common in Type 4. In the SMC, Type 1 confirmed BEL stars are almost as many as Type 4 ones, while in the LMC Type 1 ones amount to less than half of the Type 4 ones. In Sabogal et al. (2005), it is suggested that the mechanism behind the variability of Type 1 stars could depend on metallicity: in low-metallicity stars, rotation probably combined with non-radial pulsations may be the outburst's main driver, while stellar winds would have a reduced contribution. Our results with the SMC versus the LMC confirmed that BEL stars are in line with this idea.

When considering the full LMC3/SMC3 samples (that include the confirmed BEL stars), such proportions change only in the SMC, where Type 1 stars reduce even more their proportion to Type 4 ones. It must be taken into account that the Be candidate samples may have contamination from other non-Be variable stars; therefore, it is not unexpected to find some differences.

9 RED MAGELLANIC BE STARS?

Like in our previous investigation (Vieira et al. 2017), we cross-matched our clean lists of LMC 2393 and 1004 SMC Be candidates with a *Gaia* DR2 counterpart, with the IRSF catalogue by Kato et al. (2007). An easier tracking of all names and sizes of the samples used in this work can be seen in Table 5. *Gaia* DR2 2000.0 epoch coordinates were matched to the coordinates published by IRSF, and we found that true matches have angular distances distributed below

Table 3. Catalogues of spectroscopically confirmed BEL stars crossmatched with our Be candidates in the Magellanic Clouds.

Reference	Galaxy	Tables and comments about BEL confirmed stars	Number of stars matched
Martayan et al. (2007)	SMC	Table 3 (N_Star = 1 in electronic table)	7
Martayan et al. (2010)	SMC	Tables C1, C2 (Code = 1 in electronic table)	10
Paul et al. (2012)	LMC, SMC	Tables 2–7: SpT = B0–B9	2, 31
Reid et al. (2012)	LMC	Tables A1, A2: SpType = Be II to V and H_α in comments	35
Cieslinski et al. (2013)	LMC, SMC	Table 1: All except notes = 2, 3, 6, 10, 11, 14 and 15	4, 6
Sheets et al. (2013)	SMC	Table 4: those with SpT = OBe	6
Be Stars Spectra database (http://basebe.obspm.fr)	SMC	Radial velocity > 100 km s^{-1}, located in the Magellanic Clouds area	10

Table 4. Variability types of confirmed BEL and Be candidate stars in the LMC3 and SMC3 samples. Percentages with respect to the total sample being considered are shown below each line.

Confirmed BEL stars						
Sample/type	1	1/2	2	3	4	Total
LMC3	8	4	3	7	19	41
	20 %	10 %	7 %	17 %	46 %	100 %
SMC3	16	0	13	6	21	56
	29 %	0 %	23 %	11 %	37 %	100 %
Be candidate stars						
Sample/type	1	1/2	2	3	4	Total
LMC3	554	95	148	142	1170	2109
	26%	5%	7%	7%	55%	100%
SMC3	102	0	149	77	646	974
	11%	0%	15%	8%	66%	100%

Table 5. Different samples of Be candidates towards the Magellanic Clouds used in this investigation.

Sample name	LMC	SMC
Original Be candidates	2446	1019
Clean Be candidates	2393	1004
Matched with *Gaia* DR2	2393	1004
With ϖ, $\mu_\alpha \cos\delta$, and μ_δ	2357	994
Q90	2099	890
LMC1/SMC1	1856	872
LMC2/SMC2	2116	976
LMC3/SMC3	2109	974
BEL confirmed stars	41	56
Matched with IRSF	1521	737
Matched with SAGE IRAC	1882	869

0.4 arcsec, a rather small distance, within which 1521 (64 per cent of the LMC sample) and 737 (73 per cent of the SMC sample) stars were matched between these catalogues.[2] We did the same with the SAGE IRAC catalogues for the LMC and the SMC by Meixner et al. (2006) and Gordon et al. (2011), respectively. The LMC IRAC has 6 398 991 entries and the SMC one has 2 015 403 entries. These two catalogues were checked for repeated IDs or close entries within 2 arcsec on the sky, and none were found. True matches between our stars and these catalogues were all within 1 arcsec, and the obtained matches, all singles, were 1882 in the LMC (79 per cent of the sample) and 869 in the SMC (87 per cent of the sample). Not unexpectedly, some stars are missing either near-IR or mid-IR photometry or both.

Figs 10 and 11 show the optical, near- and mid-IR colour–colour diagrams for the LMC3 and SMC3 samples, highlighting confirmed BEL stars. These plots can be compared with similar or related ones in Mennickent et al. (2002), Sabogal et al. (2005), Bonanos et al. (2011), Paul et al. (2012), and Vieira et al. (2017). Among the Magellanic Be candidates, we distinguish three subsets of data that cluster or locate along some visible sequences simultaneously in different colours. We broadly define subsets A, B, and C, based on the $V-I$ versus $K-[3.6]\,\mu$m plot, in the upper mid-panel of the aforementioned figures, as follows:

(i) A: Stars with $0.0 \lesssim K-[3.6]\,\mu\text{m} \lesssim 0.2$ and $-0.2 \lesssim V-I \lesssim 0.8$. These stars occupy a vertical sequence locus with $[3.6]\,\mu\text{m}-[5.8]\,\mu\text{m} \sim 0$ in the upper right plot and a slightly tilted straight sequence in the upper left one, easily visible for $V-I > 0.3$.

(ii) B: Stars with $0.2 \lesssim K-[3.6]\,\mu\text{m} \lesssim 0.8$, which occupy an extended locus, having $-0.2 \lesssim V-I \lesssim 0.35$ and $J-K < 0.5$. These stars are in the expected location for CBe stars, as can be inferred from Hernández et al. (2005).

(iii) C: Stars with $K-[3.6]\,\mu\text{m} \gtrsim 0.0$ and $V-I \gtrsim 0.1$, which also have other near- and mid-IR colours $\gtrsim 0.5-1.0$ and are not in samples A and B.

The expected locus of CBe stars, our subset B, is very well followed by a large portion of our Magellanic Be candidates as well as our confirmed BEL stars. We find six LMC confirmed BEL stars in our subset C (ID = 531, 909, 931, 934, 1368, and 1863), which are clearly redder than CBe in all of the colours considered, except for one (ID = 934) that is exceedingly red in optical and becomes progressively less red in larger wavelength colours (black dark star symbols in Fig. 10).

Among the SMC confirmed BEL stars, we find only three of them (ID = 75, 184, and 547) that are redder than or in the redder side of CBe ones (large white star symbols in Fig. 11). More specifically, ID = 184 is redder in $J-K$ and ID = 75 and 547 are redder in $K-[3.6]\,\mu$m than CBe stars, and all three of them are among the reddest BEL stars in $J-[3.6]\,\mu$m colours, although these latter values are within the expected for CBe stars.

Table 6 lists the individually identified red confirmed BEL stars in the LMC (6) and the SMC (3), which we call *red Be stars*, indicating our ID (columns 1 and 4), identification, and spectral type listed by Reid et al. (2012) (columns 2 and 3) and by Sheets et al. (2013) (columns 5 and 6). In these references, the stars were

[2]These samples are a bit larger than the ones we found when crossmatching the SPM4 catalogue with the Be candidates in Vieira et al. (2017). Then we found 1188 and 619 matched stars in the LMC and SMC, respectively.

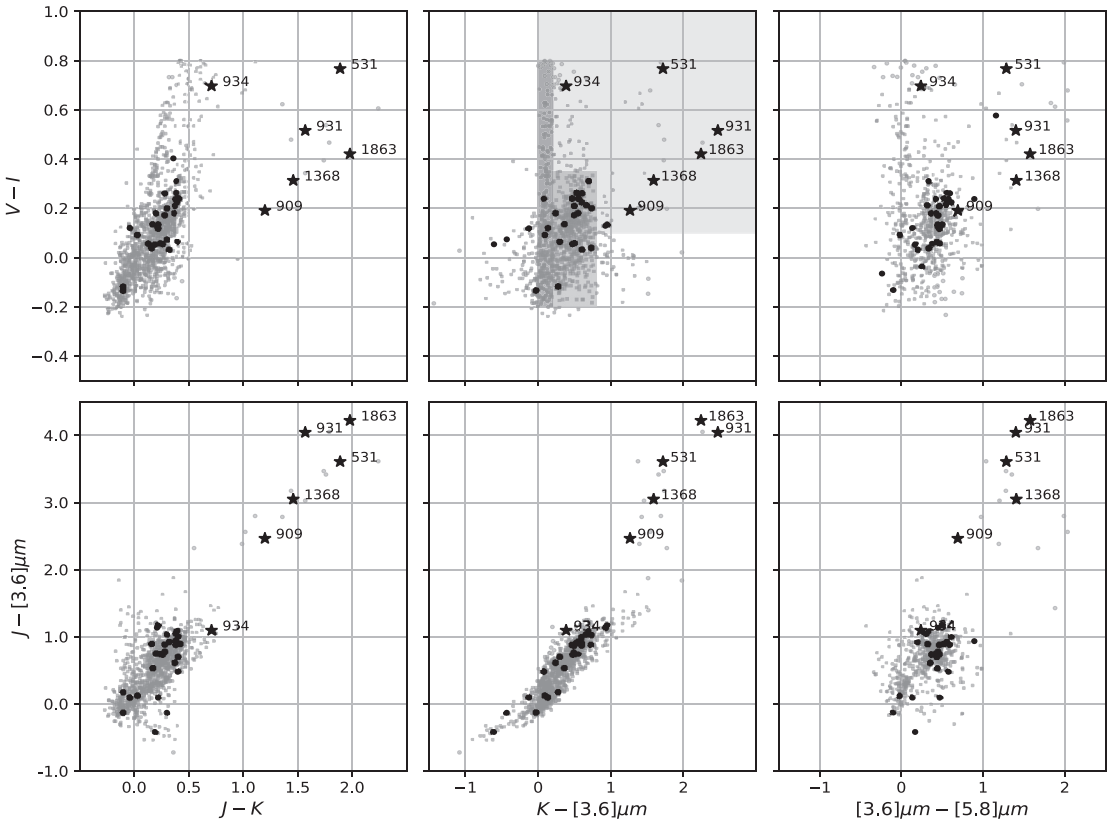

Figure 10. Optical, near- and mid-infrared colour–colour diagrams for the LMC3 sample. BEL confirmed stars are highlighted in darker symbols. Black dark star symbols are what we call red Be stars. Some stars (including BEL confirmed ones) in the LMC3 sample are missing either IRSF or IRAC photometry. The upper middle panel shows in decreasing shade grey colour, the regions corresponding to the subsets A, B, and C, respectively.

spectroscopically confirmed as BEL, since the H_α line is observed clearly in emission, although the spectra obtained were of low resolution. In this sense, these stars could also be Herbig Ae/Be (HAe/Be), B[e], or other type of emission line B star than CBe. As reported by Rivinius et al. (2013), classical Be stars can be confused with HAe/Be stars, which are pre-main-sequence objects still embedded in clouds of gas and dust and are accreting material from circumstellar discs that are by-products of the star-forming processes (Waters & Waelkens 1998). CBe stars, on the other hand, are not pre-main-sequence objects. Their circumstellar discs originate from outbursts from the star and not from an external cloud. Typically, IR and millimetric observations are used to distinguish between CBe and HAe/Be stars.

We performed a spectral energy distribution analysis to infer whether the observed IR excess for these red Be stars is produced by dust, interstellar extinction, or by thermal emission from circumstellar dust (e.g. protoplanetary disc, envelope or both). We found five red Be stars of the LMC with IR colours expected for HAe/Be. The LMC star $ID = 909$ and the three red Be stars of the SMC are not located in that region, but in an overdensity of blue stars ($B - V < 0.1$) in the colour–colour diagram, implying that they could not be HAe/Be.

On the other hand, an additional aspect observed in our results is the difference between the number of red Be stars in the LMC and the SMC. It is required to find out if this is indicative of an intrinsic difference between the BEL population of both galaxies, related, for example, to metallicity, or if it is caused by some bias/incompleteness in the available data.

In the following, we give a brief description of the four objects called here red Be stars. The SMC stars ID = 75, 184, and 547 (Type 1, Type 2, and Type 4, respectively, in the classification of Mennickent et al. 2002) were reported by Sheets et al. (2013) in table 4, and their spectra are showed in fig. 4 of that work. Those authors could not assure if the objects in their table 4 reported as OBe (stars with a clear H_α line in emission) were CBe or HAe/Be stars, because of their short ages. Although the spectra in their fig. 4 have a low resolution of 570, it is clear the presence of the H_α emission line. This is why we called them confirmed BEL stars. However, since in our analysis they cannot be classified as HAe/Be, nor discarded as CBe, it will be necessary to observe them in a medium- or high-resolution spectroscopic multiepoch follow-up to investigate their Be nature. The LMC star ID = 909 (Type 3 in the classification of Mennickent et al. 2002) was reported by Reid et al. (2012) in Table A1. The authors used low-resolution spectra for identifying the emission lines and performing the spectral classification. Then, the stars were observed with a medium resolution of 1200 to obtain radial and rotational velocities. Finally, they classified the H_α line profiles using higher resolution spectra of 8600. The spectral classification for star 909 is B3Ve, indicating that it does not present forbidden lines, it is not a supergiant, and shows the H_α line in emission. The high resolution of the stellar spectrum allows to say that this is a real emission line and not a spurious detection. Table A1 indicates that this line has a double-peaked profile with the absorption characteristic just in the centre. This implies that the star is viewed with a mid-inclination angle (Reid et al. 2012). The rotational velocity obtained in that work for star ID = 909 is 328 ± 16 km s^{-1}, that is in the range

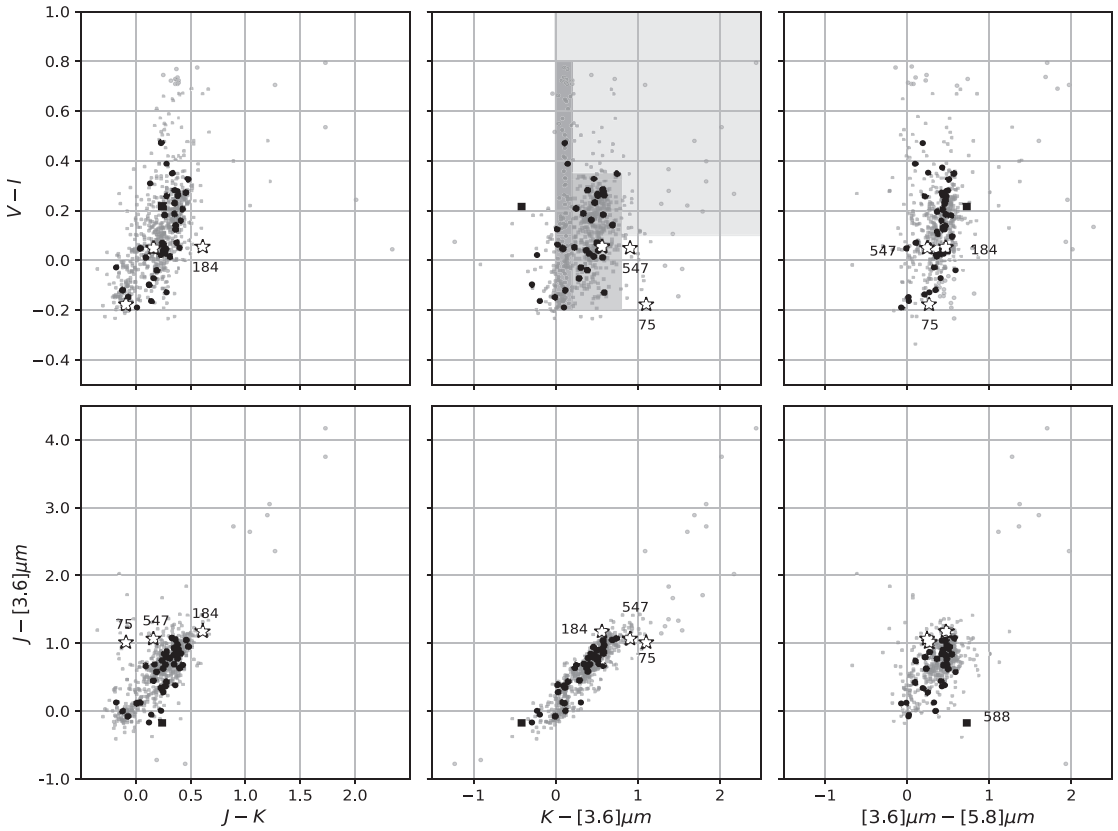

Figure 11. Optical, near- and mid-infrared colour–colour diagrams for the SMC3 sample. BEL confirmed stars are highlighted in darker symbols. Large white star symbols are stars with ID = 75, 184, and 247. Some stars (including BEL confirmed ones) in the SMC3 sample are missing either IRSF or IRAC photometry. The upper middle panel shows in decreasing shade grey colour, the regions corresponding to the subsets A, B, and C, respectively. SMC confirmed BEL star ID = 588 (black dark square symbol) is a high mass X-ray binary, which can explain its colours being visibly different from those of CBe stars.

Table 6. Magellanic red Be stars: confirmed BEL stars with redder colours than those of CBe. Stars with an asterisk could not be classified as HAe/Be.

LMC	IDR	ST	SMC	IDS	ST
531	92	B0IIIe	∗75	B103	OBe
∗909	1386	B3Ve	∗184	B081	OBe
931	1265	B8Ve	∗547	B049	OBe
934	606	B1Ve			
1368	684	B7Ve			
1863	1335	B1Ve			

of velocities of CBe. On the base of these characteristics, this star could be a Be star of the LMC. However, again, it will be necessary to observe it in a medium- or high-resolution spectroscopic multiepoch follow-up to confirm its Be nature.

Having found four red Be stars in the SMC (ID = 75, 184, and 547) and LMC (ID = 909) is an important fact that suggests that there could be more of these exceptionally red Be stars in these galaxies. Such a high reddening could be an indication of dust, which should not exist in the circumstellar environment of CBe stars, due to the high effective temperatures of their central stars. However, in case that one or more of these stars were CBe, this result would have important consequences about the physics of circumstellar discs of these stars. Further investigation is required to find the best explanation for the existence of these red Be stars in the Magellanic clouds. In the following section, we present some hypotheses to explain these red colours that exclude the idea of red CBe. These studies require additional observations and analysis.

10 ALTERNATIVE EXPLANATIONS FOR THE REDDER COLOURS OF OUR RED BE STARS

There are many possible explanations for our results than by truly red CBe stars. One of them is the possibility of stellar companions, by binarity or blending, causing redder optical and IR colours. High-resolution spectra will be needed to confirm the existence of such companion stars. Another possibility is that red Be stars in the MC belong to high-mass X-ray binary systems. The SMC confirmed BEL star ID = 588 [labelled (M2002) SMC 17703 in Martayan et al. 2010] has been identified by Haberl & Sturm (2016) as a high-mass X-ray binary (no. 45 in their table A1). It shows noticeably different colours, some bluer and some redder, than CBe stars (dark black square in Fig. 11). However, as far as we know, none of our red Be stars has been reported in a high-mass X-ray binary system.

On the other hand, another possible explanation is that a high inclined disc could produce the red colours showed by the red Be stars. We developed simulations to study this hypothesis. It has been demonstrated (Ghoreyshi et al. 2018; Rímulo et al. 2018) that a Be disc fed roughly at a constant rate, and for a sufficiently long time (a few to several years, depending on the value of the viscosity parameter α), reaches a quasi-steady state in which the density is nearly constant in time. If the gas temperature is properly taken into consideration, the density profile is typically a complicated function

of the distance from the star (Carciofi & Bjorkman 2008). However, a usual approximation is to consider the temperature of the gas to follow a power law with the radial distance, in which case the density profile assumes a power-law form given by

$$\rho(R,z) = \frac{\Sigma_0}{(2\pi)^{\frac{1}{2}}\, H_0} \left(\frac{R}{R_{\rm eq}}\right)^{-n} e^{-\frac{z^2}{2H^2}}, \quad (2)$$

where

$$H(R) = H_0 \left(\frac{R}{R_{\rm eq}}\right)^{\beta}, \ \beta = \frac{3}{2}, \quad (3)$$

is the disc scale height, and

$$H_0^2 = \frac{c_s^2}{v_{\rm orb}^2} R_{\rm eq}^2 = \frac{kT_0}{\mu m_H} \frac{R_{\rm eq}^3}{GM}. \quad (4)$$

For an isothermal disc, we must have $n = 7/2$ (Carciofi 2011). Typical values of n, however, are between 2.5 and 5 (Vieira R. G. et al. 2017). In the recent years, this simple steady-state viscous decretion disc has been successful in describing the main observed features of individual Be discs (Carciofi et al. 2006, 2007; Jones et al. 2008; Carciofi et al. 2009; Klement et al. 2015) and samples of Be stars (Silaj et al. 2010; Touhami et al. 2011; Vieira R. G. et al. 2017). We used the radiative transfer code HDUST (Carciofi et al. 2004; Carciofi & Bjorkman 2006, 2008) in order to estimate the locii of Be stars in the colour−colour diagrams presented in this work. From a grid of Be star + disc models, we generated a population of models of Be stars with parameters distributed as follows: n is uniformly distributed between 3 and 4.5; Σ_0 is uniformly distributed from 0 to 4 g cm^{-2}; M is distributed from 4.2 $M_\odot$ to 20 $M_\odot$ roughly in accordance with the mass distribution of Be stars shown in fig. 10 from Rímulo et al. (2018); W is normally distributed, with mean $\langle W \rangle = 0.81$ and standard deviation $\sigma_W = 0.12$ (Rivinius et al. 2006); and cos i is uniformly distributed between 0 and 1. All stellar models were interpolated from the grids of Georgy et al. (2014), assuming stars at the main sequence, with central hydrogen fraction given by $X_c = 0.3$. The generated population of Be star models should mimic the population of Be star candidates that are found using the variability criterion of Mennickent et al. (2002) and Sabogal et al. (2005).

In Fig. 12, we plot the obtained theoretical population of Be stars, which falls in the region B (the expected locus of Be stars). The colour of the points in the plot reflects the values of cos i. Thus, more pole-on stars tend to be redder in optical and infrared. No alignment configuration, however, is capable of producing the observed red colours of our red Be stars. Hence, the standard models cannot explain the Be star candidates of regions A and C and, particularly, the red Be stars. If future observations indeed confirm that any of our red Be stars is, in fact, a CBe star, it could be the fact that its gaseous circumstellar disc is much denser than any other previously found ($\Sigma_0 \gg 4$ g cm^{-2}). Such a dense disc, with the typical values of α viscosity parameters derived for Be stars (Ghoreyshi et al. 2018; Rímulo et al. 2018), would mean that viscous heating would not be negligible as compared to irradiated heating (Porter 1999) and the disc would contain abnormally higher temperature regions. Also, this disc would be removing much more angular momentum from the parent star, as compared to the typical values (Ghoreyshi et al. 2018; Rímulo et al. 2018), with consequences for the stellar evolution of Be stars.

On the other hand, in a study of Galactic Be stars showing far-IR excess, Miroshnichenko & Bjorkman (2000) found nine extended sources, linked probably to IR cirrus emission, i.e. patches of overdense interstellar medium heated by nearby stars (van Buren & McCray 1988). On this basis, it is possible that another explanation for our red Be stars can be that they are extended sources embedded in expanding bubbles. High-resolution images in far-IR are needed to prove this hypothesis.

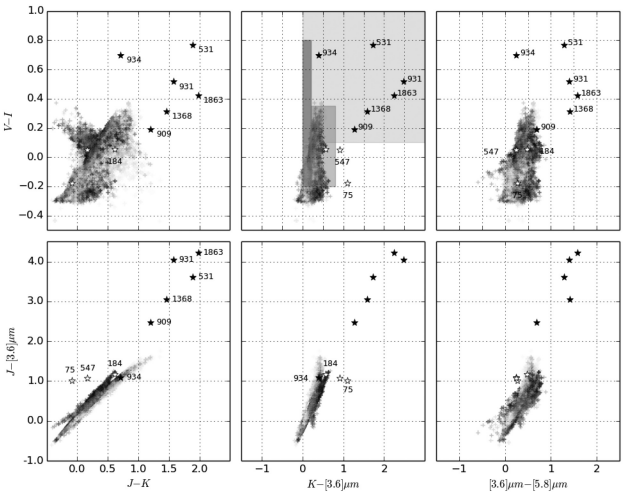

Figure 12. Theoretical population of Be stars. The colour of the points reflects the value of disc inclination cos (i): lighter shade is closer to 0 (edge-on) and darker shade in closer to 1 (pole-on). Pole-on disc stars tend to be redder, yet no alignment configuration can explain the observed red colours of our red Be stars. Red BEL stars are plotted with star symbols (black for the LMC, white for the SMC).

Finally, the IR colours and H_α emission lines observed in our red Be stars can be explained also if they are B[e] stars: BEL stars that show a large IR excess caused by a hot circumstellar dust (Miroshnichenko 2007). In their optical spectra, there are forbidden emission lines as [O$_{\rm I}$], [Fe$_{\rm II}$], [N$_{\rm II}$], and [O$_{\rm III}$], and also permitted lines as the Balmer and Fe$_{\rm II}$ (Allen & Swings 1976, Lamers et al. 1998). These forbidden emission lines and dust-type IR excess distinguish B[e] from CBe stars.

The B[e] phenomenon has been detected in supergiant (sgB[e]), pre-main-sequence (HAe/B[e]), symbiotic (SymB[e]), and FS CMa stars, as also in compact planetary nebulae (cPNB[e]). Some of the FS CMa stars could be transitional objects between binary Be and symbiotic stars (Miroshnichenko 2007). The B[e] phenomenon can be studied with different techniques: multiepoch high-resolution spectroscopy (with high S/N ratio), multicolour photometry, and spectropolarimetry. In order to study if the MC red Be stars are certainly B[e], near- and mid-IR imaging, interferometry or middle-resolution spectroscopy should be able to confirm if the emission reported by their low-resolution spectra is not spurious. Also, it may detect forbidden lines (e.g. [O$_{\rm I}$] and [Ca$_{\rm II}$]). In particular, for LMC ID = 909 star, the single-epoch high-resolution spectrum for this star reported by Reid et al. (2012) allowed to establish its spectral type and the lack of forbidden lines. Multiepoch optical and IR spectroscopy studies can confirm these results.

At last, a chance alignment within the angular resolution of OGLE and *Gaia* is not impossible but considered improbable as all four red Be stars have very similar OGLE V and *Gaia* G magnitudes, as shown by the whole sample distribution in Fig. 1.

The studies mentioned above should be carried out in order to establish the nature of our red Be stars. However, in case of not getting a conclusive result that can explain the observed red excess, perhaps a new type of objects, the red Be stars, will be waiting for an explanation of their astrophysical features and behaviour.

11 CONCLUSIONS

(i) A proper motion investigation for a sample of Be candidate stars towards the Magellanic Clouds, using data from the *Gaia* DR2 catalogue, has been done, which confirmed a previous result from Vieira et al. (2017), where a contaminant Galactic foreground population with redder colours in $B - V$ and $V - I$ was found.

(ii) Yet, thanks to the precision and accuracy of *Gaia* parallaxes and proper motions, we found that some red Be candidates do belong to the Magellanic Clouds.

(iii) Within the 2393 and 1004 Be candidates in the LMC and the SMC, respectively, we found 41 and 56 already spectroscopically confirmed B emission line stars, though those marked as Type 2 or Type 3 must be examined more carefully. All but one of these B emission line confirmed stars belong to the Magellanic Clouds. That one star was not measured by *Gaia* DR2; therefore, its membership to the Magellanic Clouds could not be assessed.

(iv) Most of our confirmed B emission line stars are Type 4, but there is a larger proportion of Type 1 versus Type 4 in the SMC than in the LMC. This is consistent with an idea put forward by Sabogal et al. (2005): eruptive Be stars are more common in metal-poorer SMC.

(v) One LMC confirmed B emission line star shows significantly redder optical, near- and mid-IR colours than what has been typically measured for Classical Be stars. For the SMC, three confirmed B emission line stars show reddish colours but not consistently in all bands. We called these four stars red Be stars, based on the fact that they are Be candidates with the H_α line in emission and colours redder than those of CBe. Some of our Be candidates, in both LMC and SMC, follow the overall redder colours trend, suggesting the existence of more Magellanic red Be stars.

(vi) The abnormal reddening of red Be stars deserves further investigation in order to clarify which kind of objects they are. Possible explanations for these red Be stars are stellar companions, remnant dust from previous evolution, bubbles in the interstellar medium, B[e] stars, among others. Further detailed investigation needs to be carried out as a follow up of this study in order to confirm or discard these hypotheses and the Be nature of these stars, in order to find the true explanation for them. If they were CBe stars, their red colours would imply that our understanding of the physics of the CBe stars and their circumstellar decretion discs would need to be reviewed, in the sense that until now, these discs have been considered free of dust due to the way in which they are formed. Infrared spectroscopic observations of these stars could be useful to discard the existence of dust in the discs.

ACKNOWLEDGEMENTS

This investigation has made use of the following software and programming language: TOPCAT (Taylor 2005) and PYTHON (Python Software Foundation, https://www.python.org/). This work has made use of data from the European Space Agency (ESA) mission *Gaia* (https://www.cosmos.esa.int/gaia), processed by the *Gaia* Data Processing and Analysis Consortium (DPAC, https://www.cosmos.esa.int/web/gaia/dpac/consortium). Funding for the DPAC has been provided by national institutions, in particular, the institutions participating in the *Gaia* Multilateral Agreement. This work has made use of the BeSS database, operated at LESIA, Observatoire de Meudon, France: http://basebe.obspm.fr. We thank the anonymous referees for their useful comments and suggestions that have improved this work. Vieira K. wants to thank the Department of Physics at Universidad de los Andes, Bogotá, Colombia, for supporting two research stays at their facilities, which made possible this investigation. García-Varela A. acknowledges financial support to this work given by Fondo de Investigaciones de la Facultad de Ciencias de la Universidad de los Andes, Colombia, through Convocatoria 2016-2 para la Financiación de proyectos de Investigación Categoría: Profesores de Planta, proyecto 'Classification of variable stars using machine-learning techniques. Sabogal B. acknowledges financial support given by Fondo de Investigaciones de la Facultad de Ciencias de la Universidad de los Andes, Colombia, through Programa de Investigación código INV-2019-84-1857. Hernández J. acknowledges support from the National Research Council of México (CONACyT) project no. 86372 and the PAPIIT UNAM project IA102921.

DATA AVAILABILITY STATEMENT

The data underlying this article are available in its online supplementary material.

REFERENCES

Allen D. A., Swings H. P., 1976, A&A, 47, 293
Arenou F. et al., 2018, 616, A17
Bonanos A. Z. et al., 2011, IAUS, 272, 264
Carciofi A. C., 2004, ApJ, 604, 238
Carciofi A. C., 2011, in Neiner C., Wade G., Meynet G., Peters G., eds, IAU Symposium, Vol. 272, Active OB Stars: Structure, Evolution, Mass Loss, and Critical Limits, p. 325
Carciofi A. C., Bjorkman J. E., 2006, ApJ, 639, 1081
Carciofi A. C., Bjorkman J. E., 2008, ApJ, 684, 1374
Carciofi A. C., et al., 2006, ApJ, 652, 1617
Carciofi A. C., Magalhães A. M., Leister N. V., Bjorkman J. E., Levenhagen R. S., 2007, ApJ, 671, L49
Carciofi A. C., Okazaki A. T., Le Bouquin J. B., Štefl S., Rivinius T., Baade D., Bjorkman J. E., Hummel C. A., 2009, A&A, 504, 915
Cieslinksi D., Diaz M., Mennickent R. E., Kolaczkowski Z, Pereira C., 2013, IBVS, 6088 (C13)
Collins G. W. II., 1987, In IAU Colloq. 92: Physics of Be stars, p. 3
Evans M., Hastings N., Peacock B., 2000, Statistical Distributions, 3rd ed., Wiley, New York
Feigelson E. D., Babu G. J., 2012, 'Modern Statistical Methods for Astronomy'. Cambridge University Press, New York
Gaia Collaboration, 2016, A&A, 595, A1
Gaia Collaboration, 2018a, A&A, 616, A1
Gaia Collaboration, 2018b, A&A, 616, A12
Galadí-Enríquez D., Jordi C., Trullols E., 1998, A&A, 337, 125
Georgy C., Granada A., Ekström S., Meynet G., Anderson R. I., Wyttenbach A., Eggenberger P., Maeder A., 2014, A&A, 566, A21
Ghoreyshi M. R., et al., 2018, MNRAS, 479, 2214
Girard T. M. et al., 2011, AJ, 142, 15
Gordon K. D. et al., 2011, AJ, 142, 102
Gyuk G., Dalal N., Griest K., 2000, AJ, 535, 90
Haberl F., Sturm R., 2016, A&A, 586, A81
Heiberger R. M., Holland B., 2012, Statistical Analysis and Data Display, second ed. Springer, New York
Hernández J., Calvet N., Hartmann L., Briceño C., Sicilia-Aguilar A., Berlind P., 2005, AJ, 129, 856
Heumann C., Schomaker G. J., Shalabh, 2016, Introduction to Statistics and Data Analysis. Springer, Switzerland
Jones C. E., Tycner C., Sigut T. A. A., Benson J. A., Hutter D. J., 2008, ApJ, 687, 598
Kato D. et al., 2007, PASJ, 59, 615
Klement R. et al., 2015, A&A, 584, A85
Lamers H. J. G. L. M., Zickgraf F.-J., de Winter D., Houziaux L., Zorec J., 1998, A&A, 340, 117
Luri X. et al., 2018, A&A, 616, A9

Luri X., on behalf of Gaia DPAC, 2019, in Montesinos B., Asensio Ramos A., Buitrago F., Schödel R., Villaver E., Pérez-Hoyos S., Ordóñez-Etxeberria I., eds, Highlights on Spanish Astrophysics X, Proceedings of the XIII Scientific Meeting of the Spanish Astronomical Society held on July 16-20, 2018, Salamanca, Spain, p. 16
Martayan C., Baade D., Fabregat J., 2010, A&A, 509, A11
Martayan C., Fremat Y., Hubert A.-M., Floquet M., Zorec J., Neiner C., 2007, A&A, 462, 683
Meixner M. et al., 2006, AJ, 132, 2268
Mennickent R. E., Pietrzyński G., Gieren W., Szewczyk O., 2002, A&A, 393, 887
Miroshnichenko A. S., 2007, ApJ, 667, 497
Miroshnichenko A. S., Bjorkman K. S., 2000, in Smith M. A., Henrichs H. F., Fabregat J., eds, ASP Conf. Ser. Vol. 214, IAU Colloq. 175: The Be Phenomenon in Early-Type Stars. Astron. Soc. Pac., San Francisco, CA, p. 484
Patel J. K., Read C. B., 1996, Handbook of the Normal Distribution. Marcel Dekker Inc., New York
Paul K. T., Subramaniam A., Mathew B., Mennickent R. E., Sabogal B., 2012, MNRAS, 421, 3622
Porter J. M., 1999, A&A, 348, 512
Reid W. A., Parker Q. A., 2012, MNRAS, 425, 355
Rímulo L. R. et al., 2018, MNRAS, 476, 3555
Rivinius T., Carciofi A. C., Martayan C., 2013, A&A Rev., 21, 69
Rivinius T., Štefl S., Baade D., 2006, A&A, 459, 137
Sabogal B. E., Mennickent R. E., Pietrzinsky G., Gieren W., 2005, MNRAS, 361, 1055
Sheets H. et al., 2013, A&A, 711, 111
Silaj J., Jones C. E., Tycner C., Sigut T. A. A., Smith A. D., 2010, ApJS, 187, 228
Stassun K. G., Torres G., 2018, ApJ, 862, 61
Taylor M. B., 2005, ASP Conf. Ser., 347, 29
Touhami Y., Gies D. R., Schaefer G. H., 2011, ApJ, 729, 17
van Buren D., McCray R., 1988, ApJ, 329, L93
Vasilevskis S., Klemola A., Preston G., 1958, AJ, 63, 387
Vieira K. et al., 2010, AJ, 140, 1934
Vieira K., García-Varela A., Sabogal B., 2017, MNRAS, 469, 4175
Vieira R. G., Carciofi A. C., Bjorkman J. E., Rivinius T., Baade D., Rímulo L. R., 2017, MNRAS, 464, 3071
Waters L. B. F. M., Waelkens C., 1998, ARA&A, 36, 233
Zinn J. C., Pinsonneault M. H., Huber D., Stello D., 2019, AJ, 878, 136

SUPPORTING INFORMATION

Supplementary data are available at *MNRAS* online.

catalog_LMC_all_data.txt (2393 stars)
catalog_red_be_stars.txt (4 stars)
catalog_SMC_all_data.txt (1004 stars)

Please note: Oxford University Press is not responsible for the content or functionality of any supporting materials supplied by the authors. Any queries (other than missing material) should be directed to the corresponding author for the article.

APPENDIX A: TABLES

A sample of the LMC data used in this investigation is shown below (Table A1). Table A2 shows the same data for our four red Be stars. Full tables (one for the LMC, one for the SMC, and one for the four red Be stars that has stars from both Clouds) are available as online supplementary material.

Table A1. Sample of the LMC data used in this investigation. It includes OGLE-II ID and BVI photometry, Variability Type (Type = 1.5 is for Type 1/2, i.e. sharing both values); *Gaia* DR2 source ID, coordinates, parallax and proper motions with their errors, and BGR photometry; our posmag_ranking and χ-value for membership to the Clouds; other names for the BEL confirmed stars only (set to – when no name was given) as listed in the references in Table 3; IRSF JHKs photometry; and IRAC [3.6, 4.5, 5.8, 8.0] μm photometry for each star.

This paper ID	OGLE-II ID	V (mag)	$B-V$ (mag)	$V-I$ (mag)	Variab. Type	*Gaia* DR2 source ID	α (deg)	δ (degrees)	ϖ (mas)	ϵ_{ϖ} (mas)	$\mu_\alpha \cos(\delta)$ (mas yr^{-1})	$\epsilon_{\mu_\alpha \cos(\delta)}$ (mas yr^{-1})
1	05071018-6910538	16.899	−0.074	0.006	1.0	4661232628032602752	76.79218055039	−69.18158550247	−0.2078	0.0752	1.634	0.171
2	05123453-6914375	14.3	−0.125	−0.082	1.0	4658240753888659456	78.14363046873	−69.24371968086	−0.0796	0.1736	2.479	0.242
3	05173303-6920189	17.478	0.048	0.129	1.0	4658192233605799808	79.38731184581	−69.33854593851	−0.0421	0.1078	1.848	0.17
4	05023318-6921184	16.015	−0.068	−0.043	1.0	4655233138520014592	75.63790883973	−69.35504535077	0.046	0.0403	1.894	0.077
5	05200092-6941138	17.986	0.077	0.18	1.0	4658166223321197312	80.00338154581	−69.68713050128	0.0552	0.1437	1.919	0.206
6	05200237-6927100	16.227	−0.124	−0.082	1.0	4658175435947436288	80.00947440419	−69.45277712703	−0.0887	0.0663	2.085	0.109
7	05200385-6948340	17.07	−0.23	0.007	1.0	4658140904452708736	80.01579285108	−69.80935793508				
8	05200424-6925374	15.661	−0.162	−0.14	1.0	4658176947831707008	80.01727024206	−69.42705739503	0.1395	0.0678	2.656	0.109
9	05200714-6939426	14.656	−0.015	0.172	1.0	4658166399388690688	80.02930474084	−69.66182328727	−0.046	0.0873	1.643	0.134
10	05223928-6952325	16.317	0.307	0.662	1.0	4657972399949681920	80.66322850573	−69.87567345694	8.0E-4	0.0375	2.072	0.066
	⋮											
25	05173037-6920349	16.625	0.002	−0.082	2.0	4658192203563908992	79.37610453534	−69.34299613095	−0.1427	0.0958	1.801	0.149
26	05173364-6921328	16.356	−0.04	−0.065	2.0	4658191344570530816	79.38986687638	−69.35906390055	0.0163	0.0596	2.28	0.085
27	05300135-6928099	15.776	−0.207	0.238	3.0	4658043249748073472	82.50530387206	−69.46940253938	−0.3151	0.2066	0.887	0.336
28	05390419-7005011	16.499	−0.172	0.049	3.0	4657251021605219968	84.76693210448	−70.08363577666	−0.0461	0.0542	2.088	0.095
29	05045870-6910069	16.546	0.043	0.292	4.0	4661244374880374400	76.24436119511	−69.16850244506	−0.0885	0.066	2.005	0.109
30	05050594-6910449	15.431	−0.02	0.215	4.0	4661244306027427584	76.27448372936	−69.17911023874	0.0985	0.0469	1.788	0.087

Table A1. - continued.

μ_δ (mas yr^{-1})	ϵ_{μ_δ} (mas yr^{-1})	B (mag)	G (mag)	R (mag)	posmag_ranking value	χ value	BEL confirmed other names	J (mag)	H (mag)	Ks (mag)	[3.6] μm (mag)	[4.5] μm (mag)	[5.8] μm (mag)	[8.0] μm (mag)
−0.006	0.182	16.763409	16.642477	16.630665	0.160	1.857					17.05			
2.137	0.318	14.250258	14.057608	14.143691	0.101	2.322		14.6	14.67	14.71				
0.424	0.218	17.37947	17.182137	16.957771	0.146	0.268					16.454	16.05		
−0.043	0.097	16.013058	15.887163	16.052021	0.130	1.650		15.99	15.95	15.94	15.674	15.475		
0.013	0.293	18.011503	17.789316	17.532957	0.154	0.493								
0.251	0.169	16.270792	16.122494	16.257172	0.141	1.021						16.126		
		17.001675			0.126						14.076	14.156	13.862	
0.862	0.158	15.637781	15.453746	15.601172	0.139	3.221		15.61	15.53	15.42	15.131	14.974	14.662	
0.221	0.195	14.799377	14.578164	14.678681	0.204	0.642					13.46	13.221	13.048	
0.304	0.081	16.198282	16.35375	15.715758	0.188	1.129		15.09	14.64	14.52	14.389	14.454	14.621	
		⋮												
0.243	0.197	16.738895	16.383902	16.215532	0.188	0.895								
−0.091	0.116	16.397356	16.263079	16.30308	0.119	2.140		16.17	16.21	16.17	15.696	15.626		
0.222	0.481	15.477867	15.366205	15.004803	0.316	1.395	RP_786				13.731	13.576	13.307	13.1
0.566	0.108	16.632305	16.523197	16.450397	0.217	1.279		15.98	15.77	15.45	14.918	14.578	14.131	
0.013	0.146	16.55129	16.427717	16.406654	0.105	1.126		16.77	16.72	16.55				
0.126	0.111	15.432999	15.337342	15.413625	0.095	1.721		15.32	15.26	14.96	14.355	14.184	13.855	13.717

Table A2. Same table as before, but only the four red Be stars are included. ID = 909 is in the LMC and ID = 75, 184, and 547 are in the SMC.

This paper ID	OGLE-II ID	V (mag)	$B-V$ (mag)	$V-I$ (mag)	Variab. Type	*Gaia* DR2 Source ID	α (deg)	δ (deg)	ϖ (mas)	ϵ_{ϖ} (mas)	$\mu_{\alpha}\cos(\delta)$ (mas yr^{-1})	$\epsilon_{\mu_{\alpha}\cos(\delta)}$ (mas yr^{-1})
909	05163930-6920482	17.21	−0.079	0.191	3	4658189351701024896	79.16335801642	−69.34666821498	0.2341	0.0816	1.637	0.142
75	005504.55-724637.3	14.156	−0.111	−0.178	1	4685982806630491648	13.76896086484	−72.7770997258	0.0447	0.0325	0.792	0.067
184	005206.05-725208.7	15.961	−0.148	0.054	2	4685959403340845312	13.02528552346	−72.8692141688	−0.055	0.0394	0.581	0.079
547	004942.75-731717.7	14.453	−0.115	0.049	4	4685931679327948800	12.42810225874	−73.28838419448	−0.1164	0.0314	0.356	0.054

Table A2. - continued.

μ_δ (mas yr^{-1})	ϵ_{μ_δ} (mas yr^{-1})	B (mag)	G (mag)	R (mag)	posmag_ranking value	χ value	BEL confirmed other names	J (mag)	H (mag)	Ks (mag)	[3.6] μm (mag)	[4.5] μm (mag)	[5.8] μm (mag)	[8.0] μm (mag)
−0.104	0.183	17.15636	16.814718	16.611889	0.14827046694154847	2.2372665627995842	SAB899	16.49	15.95	15.29	14.026	13.592	13.335	13.088
−1.274	0.052	14.16928	40.3053	14.307247	0.12046620512225799	1.697884385478025	smc1-17, B103	14.56	14.6	14.65	13.548	13.413	13.281	13.046
−1.111	0.064	15.766048	61.8202	15.724222	0.30135290880066146	1.2536129357415433	B081	15.67	15.37	15.06	14.498	14.204	14.026	13.599
−1.096	0.051	14.462686	162.339	14.502104	0.23370929985365374	3.831751691002231	B049	14.47	14.39	14.31	13.405	13.225	13.162	13.034

This paper has been typeset from a TEX/LATEX file prepared by the author.